Supplemental Material

Polyglutamine expansion alters the dynamics and molecular architecture of aggregates in dentatorubropallidoluysian atrophy

Justyna Hinz, Lothar Lehnhardt, Silke Zakrzewski, Gong Zhang, Zoya Ignatova

From the Institute of Biochemistry and Biology, University of Potsdam, 14467 Potsdam, Germany

Running title: *Dynamics of DRPLA aggregates*

Supplemental Materials and Methods

Immunoprecipitation, two-dimensional gel analysis and mass spectrometry – Cells fractionated into nuclear and cytoplasmic fractions as described above were immunoprecipitated with anti-GFP antibodies according to the manufacturer's instructions (MicroBeads, Miltenyi), resuspended in 50 µl DeStreak rehydration solution (GE Healthcare) before being separated on 7-cm Immobiline DryStrip Gels, non-linear pH range 3-10 (GE Healthcare). In the second dimension, samples were separated on 10% SDS-PAGE and Coomassie stained (36). Protein spots identified for further analysis were excised and digested with 30 ng/µl trypsin sequencing grade (Roche) at 37 °C for 12 h and identified by MALDI-TOF MS (microflex LRF, Bruker Daltonics). Protein identification was performed using SwissProt database.

Supplemental Table S1. Quantification of the localization pattern of GFP-ATN1 variants. Cells expressing FL-ATN1 and ΔN-ATN1 proteins were counted in blind experiments for the presence of inclusions and diffusive staining of nucleus and cytoplasm.

Protein	Time of expression, h	Nuclear localization		Cytoplasmic localization	
		Diffuse distribution, %	Hyperfluorescent loci, %	Diffuse distribution, %	Hyperfluorescent loci, %
FL19Q	24	74 ± 4	26 ± 4	93 ± 3	5 ± 1
	48	36 ± 3	63 ± 4	73 ± 2	29 ± 4
FL71Q	24	34 ± 5	65 ± 4	48 ± 4	51 ± 3
	48	23 ± 4	77 ± 5	38 ± 5	61 ± 5
ΔN19Q	24	n.d.	n.o.	22 ± 4	78 ± 4
	48	n.d.	n.o.	20 ± 6	80 ± 6
ΔN71Q	24	n.d.	n.o.	21 ± 3	79 ± 3
	48	n.d.	n.o.	21 ± 4	79 ± 4

n.o., not observed; n.d., not determined

Supplemental Table S2. MALDI-TOF analysis of FL71Q and FL19Q inclusions. The mobile fraction was calculated from the FRAP measurements and the half-life time from the iFRAP experiments. The standard deviation is a mean value of the analysis in three to ten cells.

Protein	Localization	Expression time, h	FRAP	iFRAP
			Mobile Fraction, %	Half-life time, min
FL19Q	nucleus	24	87.6 ± 12.2	48 ± 7
		48	78.4 ± 16.3	182 ± 74
	cytoplasm	24	13.5 ± 7.4	−
		48	14.7 ± 9.6	−
FL71Q	nucleus[a]	24	79.6 ± 19.0	110 ± 13
		48	64.9 ± 14.5	206 ± 73
	nucleus[b]	24	30.6 ± 7.7	1440 ± 212
		48	28.1 ± 9.1	2937 ± 860
	cytoplasm	24	13.6 ± 6.8	−
		48	13.8 ± 4.4	−
ΔN19Q	cytoplasm	24	17.6 ± 5.2	−
		48	16.8 ± 4.3	n.d.
ΔN71Q	cytoplasm	24	15.7 ± 5.5	−
		48	11.1 ± 4.4	n.d.

FL71Q protein from two distinct aggregate types in the nucleus: high-recovering ([a]) and low-recovering ([b]) species in the FRAP experiments; '−' non-decaying species; n.d., not determined.

Supplemental Table S3. Proteins with aberrant association patterns in the FL71Q aggregates as compared to the corresponding FL19Q inclusions. Proteins that were specifically influenced by the nuclear FL71Q aggregates were classified into two groups: depleted and enriched in the FL71Q aggregates as compared to the FL19Q inclusions.

Aggregate type	Compared to FL19Q		Protein	Cellular function
nuclear FL71Q	enriched	1	Nucleolin	Pre-rRNA transcription and ribosome biogenesis
	enriched	2	Chromosomal protein 1A	Chromosome cohesion and DNA repair
	enriched	3	Heterogeneous nuclear protein L	Component of the heterogeneous nuclear ribonucleoprotein (hnRNP)
	depleted	4	Nuclear ribonucleoprotein G	Pre-mRNA splicing
cytoplasmic FL71Q	depleted	5	Endoplasmin (murine Hsp90)	Molecular chaperone
	depleted	6	Heat shock cognate Hsp protein 90β	Molecular chaperone

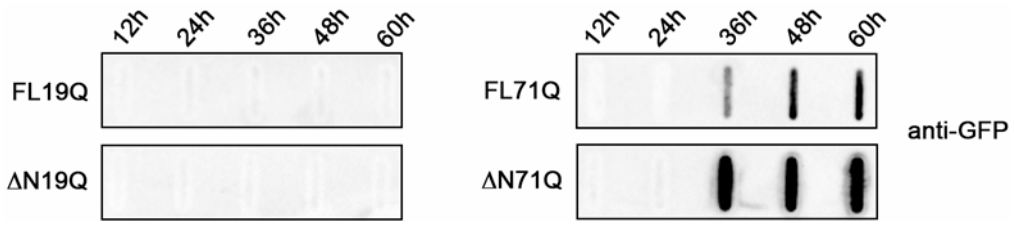

Supplemental Figure S1. FL-ATN1 and ΔN-ATN1 with expanded polyQ tracts form detergent-resistant aggregates. N2a/Tet-Off cells expressing each protein at different times were lysed and applied to the cellulose acetate membrane, washed with SDS-containing buffer and probed with anti-GFP antibodies. Total cell lysates (cytoplasmic and nucleoplasmic fraction) from equal cell numbers were loaded onto the membrane for each time point.

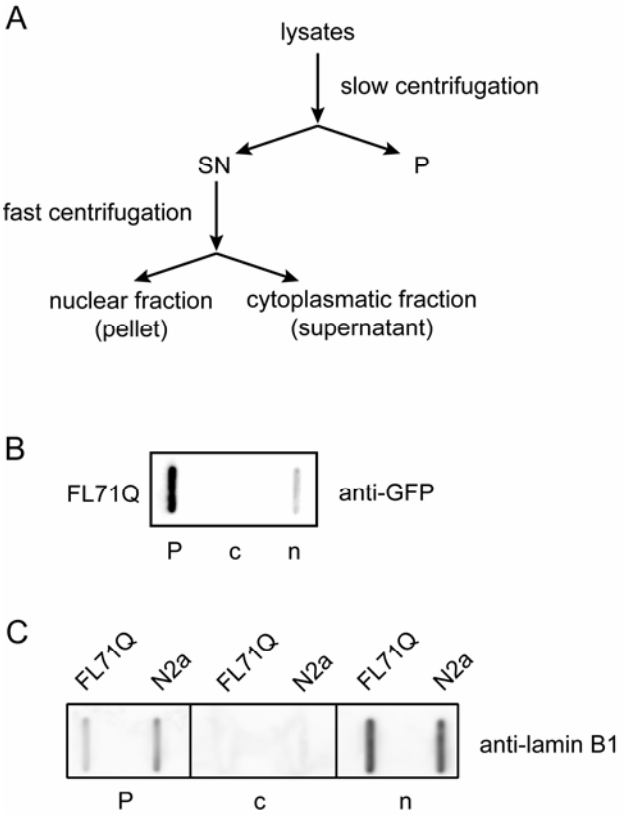

Supplemental Figure S2. Nuclear and cytoplasmic FL71Q aggregates contain detergent-resistant species. (A) Five million N2a/Tet-Off cells expressing FL71Q for 48 h were fractionated into nucleoplasmic (n) and cytoplasmic (c) fractions. SN, supernatant, P, low-speed sedimenting pellet fraction. (B) Analysis of the FL71Q fractions for detergent resistance using filter-retardation assay. The fractions in panel A were applied to the cellulose acetate membrane, washed with SDS-containing buffer and probed with anti-GFP antibodies. (C) Counterstaining of the fractions with anti-lamin B1 (1:1000, Abcam) antibodies (note, here nitrocellulose membrane is used which retains all proteins). Large aggregates co-sedimented at low velocity into the P fraction which contains cell debris and a small fraction of intact cells (the latter is responsible for the low positive lamin B1 signal). Mock-transfected N2a/Tet-Off cells (N2a) were used as a control. SN, supernatant.

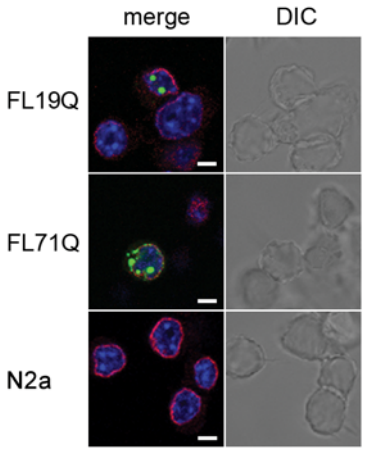

Supplemental Figure S3. Nuclear and cytoplasmic FL71Q inclusions do not alter lamin B1 distribution. N2a/Tet-Off cells were transiently transfected with FL19Q or FL71Q and visualized by the GFP fluorescence after 24 h. Nuclei were counterstained with DAPI and the nuclear envelope with anti-lamin B1 (1:1000, Abcam) antibody and Alexa-568 labeled secondary antibody (red channel). Mock transfected N2a/Tet-Off cells (N2a) served as a control. Scale bar, 5μm.

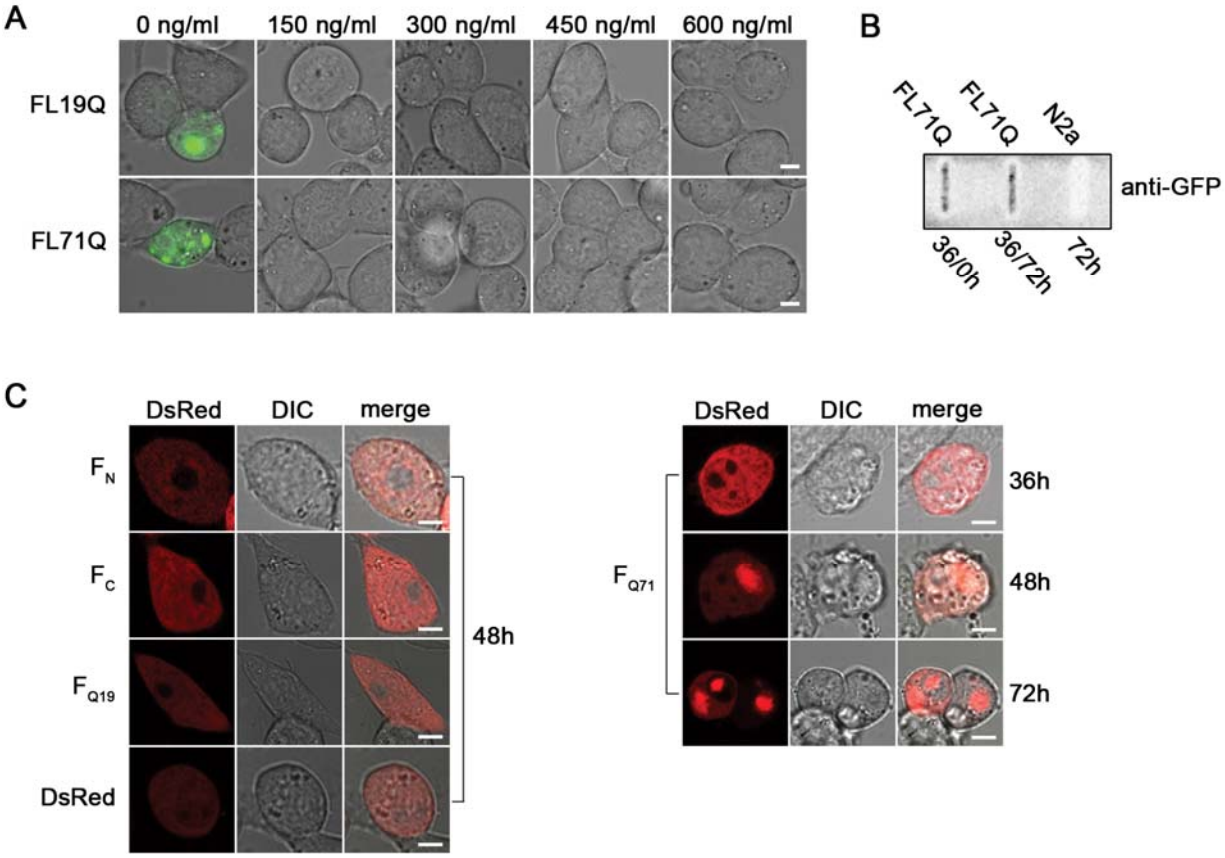

Supplemental Figure S4. Controls of the *in vivo* cross-seeding experiment. (A) Addition of doxacyclin tightly inhibited the pTRE-promoter-controlled protein synthesis. FL19Q and FL71Q were transfected into N2a/Tet-Off/LacI cells and the *de novo* synthesis was inhibited by addition of different concentrations of doxacyclin (denoted over the images). Cells were analyzed after 36 h. Scale bar, 5 µm. (B) Filter-retardation assay of N2a/Tet-Off/LacI cells expressing FL71Q protein for 36 h compared to the mock-transfected N2a/Tet-Off/LacI empty cells (N2a). The times 36/0h and 36/36h denote the expression time of FL71Q (36 h) followed by the time of analysis (0 or 36h) after the inhibition of the *de novo* FL71Q synthesis with 300 ng/ml doxacyclin. The unchanged intensity of the aggregates indicates that the amount of the SDS-resistant FL71Q aggregates did not change with the time of expression of the fragments in Figs. 4, 5. (C) ATN1 fragments remained soluble during the cross-seeding cycle. F_N, F_C, F_{Q19} and F_{Q71} fragments (see the schematic in Fig. 4A) were transfected in N2a/Tet-Off/LacI cells and their expression was induced by adding IPTG. The expression time is indicated at the right of each image series. Cells were visualized using a confocal microscope with 561-nm laser wavelength for DsRed and differential interference-contrast microscopy (DIC). The fragment F_{Q71} formed aggregates in a time-dependent manner (right panel), whereas all other fragments showed a diffuse staining accounting for a soluble expression (left panel). Therefore, the expression of the ATN1 fragments in the cross-seeding experiment was limited to 24 h, at which all fragments, including F_{Q71}, were present in a soluble state. Note that all fragments partitioned between the nucleus and cytosol despite the lack of a NLS sequence. Scale bar, 5.5 µm.

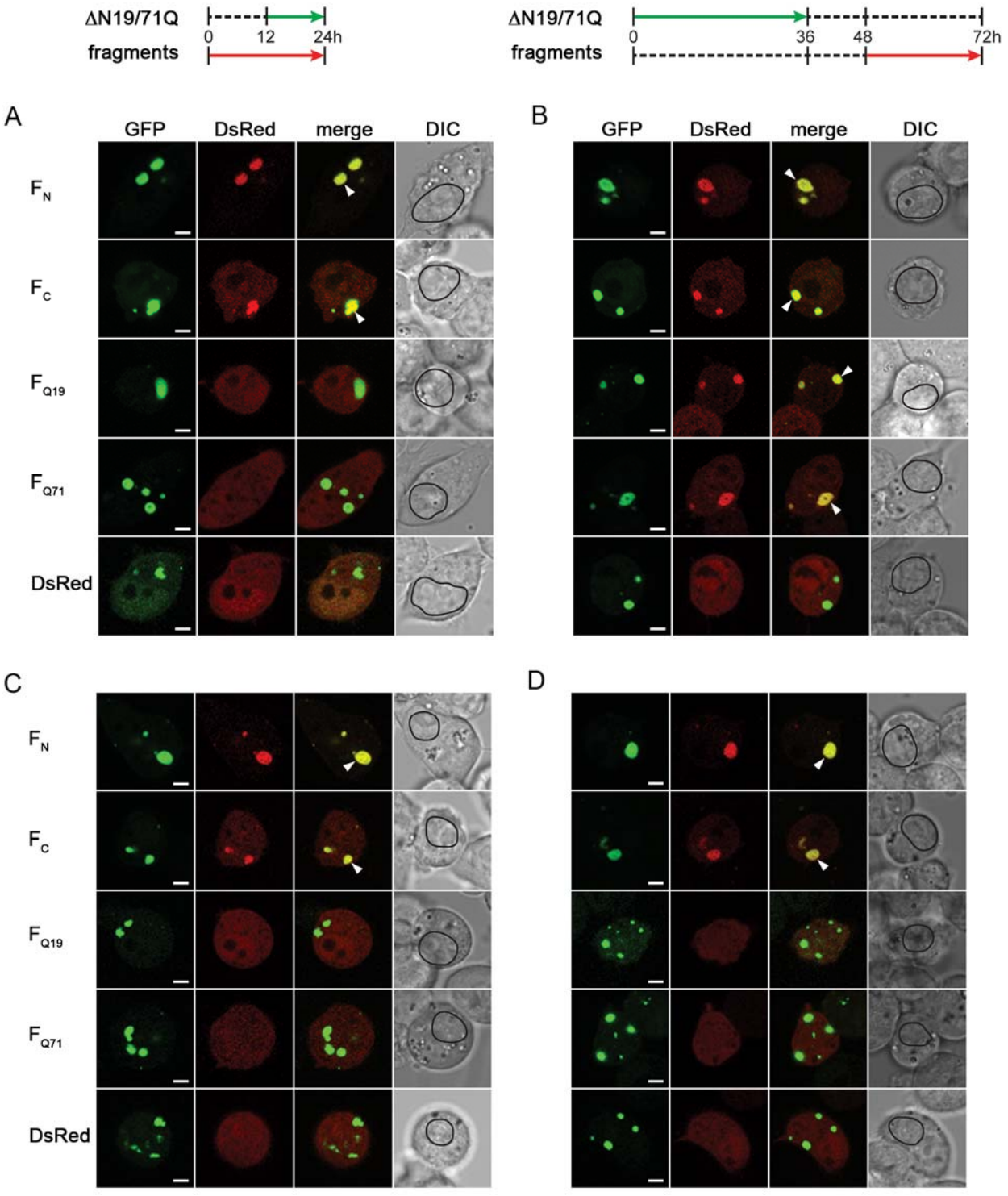

Supplemental Figure S5. Orthogonal cross-seeding of ΔN19Q and ΔN71Q inclusions with the ATN1 fragments. (A,B) ΔN71Q aggregates recruited F_N and F_C fragments at early (A) and F_{Q19} and F_{Q71} at later times of expression (B). (C,D) Cytoplasmic ΔN19Q inclusions recruited only F_N and F_C fragments at early (C) and late expression times (D). For details refer to Fig. 5.

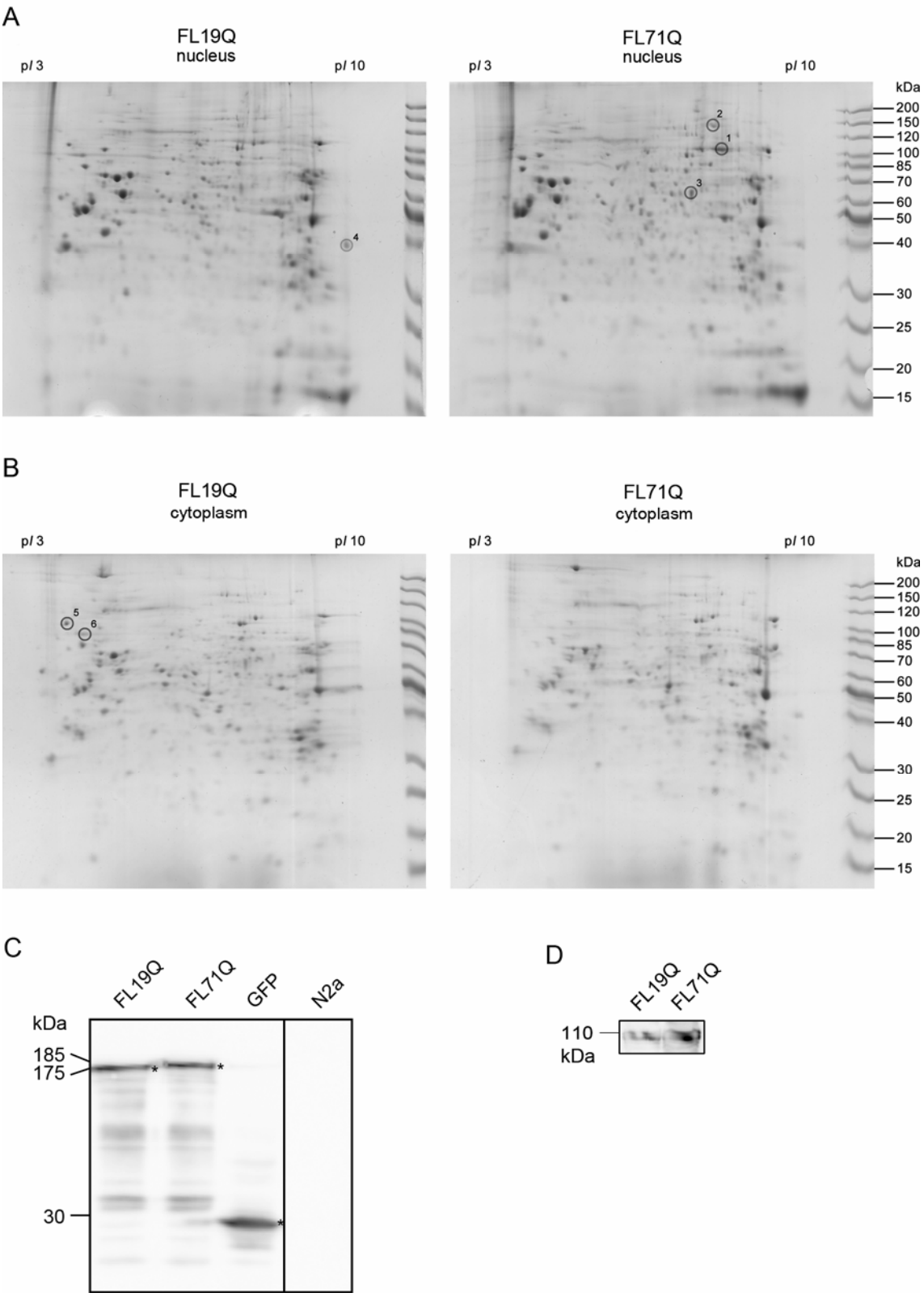

Supplemental Figure S6. Identification of the ATN1 aggregates-associated proteins. FL19Q or FL71Q were transiently expressed in N2a/Tet-Off cells for 48 h, the nuclear (A) and cytoplasmic

(B) fraction was isolated as described in Fig. S2A and proteins associated with the inclusions were immunoprecipitated with anti-GFP antibody and analyzed on 2D-gels. Proteins enriched in the nuclear FL71Q aggregates are circled on the right panel; proteins depleted in the nuclear FL71Q inclusions are marked on the left panel; and those depleted in cytoplasmic FL71Q aggregates were depicted in (B) on the left panel. The numbers of the spots correspond to the numbers in the Table 3. (C) Specificity of the immunoprecipitation of the FL-ATN1 aggregates (panels A and B) with the anti-GPF antibodies. N2a/Tet-Off cells expressing FL19Q or FL71Q for 48 h were lysed and subjected to immunoprecipitation with anti-GFP antibody-coupled magnetic beads. Immunoprecipitants were resuspended in Laemmli buffer and analyzed by immunoblot stained with anti-GFP antibodies. The dominating GFP-tagged FL19Q and FL71Q bands suggest the specificity of the immunoprecipitation. The lower, GFP-positive bands are probably degradation products of FL-ATN1 during the processing of the samples. GFP expressing cells and mock-transfected N2a/Tet-Off (N2a) were used as a control. Bands corresponding to the FL19Q, FL71Q and GFP are highlighted with an asterisk on each lane. (D) The nucleoplasmic fraction of FL71Q (panel A) was immunoprecipitated and analyzed by immunoblot with anti-nucleolin (1:1000, Abcam) antibodies. Note that there are two nucleolin-positive bands most likely representing the two alternatively phosphorylated forms of the full-length protein.